The EMBO Journal (2004) 23, 2674–2683 | © 2004 European Molecular Biology Organization | All Rights Reserved 0261-4189/04
www.embojournal.org

THE EMBO JOURNAL

Mdc1 couples DNA double-strand break recognition by Nbs1 with its H2AX-dependent chromatin retention

Claudia Lukas[1], Fredrik Melander[1], Manuel Stucki[2], Jacob Falck[1,2], Simon Bekker-Jensen[1], Michal Goldberg[2,4], Yaniv Lerenthal[3], Stephen P Jackson[2], Jiri Bartek[1] and Jiri Lukas[1,*]

[1]Danish Cancer Society, Institute of Cancer Biology, Copenhagen, Denmark, [2]Wellcome Trust/Cancer Research UK Gurdon Institute, Department of Zoology, Cambridge University, Cambridge, UK and [3]Department of Human Genetics and Molecular Medicine, Sackler School of Medicine, Tel Aviv University, Ramat Aviv, Israel

Mdc1/NFBD1 controls cellular responses to DNA damage, in part via interacting with the Mre11–Rad50–Nbs1 complex that is involved in the recognition, signalling, and repair of DNA double-strand breaks (DSBs). Here, we show that in live human cells, the transient interaction of Nbs1 with DSBs and its phosphorylation by ATM are Mdc1-independent. However, ablation of Mdc1 by siRNA or mutation of the Nbs1's FHA domain required for Mdc1 binding reduced the affinity of Nbs1 for DSB-flanking chromatin and caused aberrant pan-nuclear dispersal of Nbs1. This occurred despite normal phosphorylation of H2AX, indicating that lack of Mdc1 does not impair this DSB-induced chromatin change, but rather precludes the sustained engagement of Nbs1 with these regions. Mdc1 (but not Nbs1) became partially immobilized to chromatin after DSB generation, and siRNA-mediated depletion of H2AX prevented such relocalization of Mdc1 and uncoupled Nbs1 from DSB-flanking chromatin. Our data suggest that Mdc1 functions as an H2AX-dependent interaction platform enabling a switch from transient, Mdc1-independent recruitment of Nbs1 to DSBs towards sustained, Mdc1-dependent interactions with the surrounding chromosomal microenvironment.

The EMBO Journal (2004) **23,** 2674–2683. doi:10.1038/sj.emboj.7600269; Published online 17 June 2004
Subject Categories: genome stability & dynamics
Keywords: cell cycle checkpoints; DNA damage; live-cell imaging; Mdc1; Nbs1

Introduction

To prevent irreversible damage to genome integrity following the generation of DNA double-strand breaks (DSBs), eukaryotic cells activate genome-surveillance signalling cascades initiated by activation of the ATM (ataxia-telangiectasia-mutated) protein kinase (Bakkenist and Kastan, 2003; Shiloh, 2003). One of the key effectors of the ATM-regulated DNA damage response is the evolutionarily conserved Mre11–Rad50–Nbs1 (MRN) complex (D'Amours and Jackson, 2002; Petrini and Stracker, 2003; van den Bosch *et al*, 2003) involved in nucleolytic processing of DNA ends, recombination, repair, and checkpoint signalling. The prominent role of MRN in ATM-controlled genome surveillance is illustrated by the fact that deficiency of any of its components recapitulates some of the key defects (such as chromosomal fragility, radiosensitivity, and genetic instability) observed in cells derived from ataxia-telangiectasia (A-T) patients (Tauchi *et al*, 2002). Despite all MRN components might be phosphorylated after DNA damage, the best-characterized event is ATM-mediated phosphorylation of Nbs1 (Dong *et al*, 1999; Kim *et al*, 1999; Gatei *et al*, 2000; Lim *et al*, 2000; Zhao *et al*, 2000). One established (yet mechanistically poorly characterized) function of this phosphorylation is inhibition of DNA replication in response to ionizing radiation (IR), and failure to activate this mechanism (so-called intra-S-phase checkpoint) leads to radio-resistant DNA synthesis (RDS) (Painter and Young, 1980). Whether and how phosphorylation of Nbs1 and/or additional MRN components contribute to other functions of this important DSB-associated enzyme is not clear.

A more recently identified role of Nbs1 and Mre11 involves their ability to facilitate the activation of ATM after low doses of IR and/or radiomimetic drugs (Carson *et al*, 2003; Uziel *et al*, 2003; Horejsi *et al*, 2004). However, the key issue of how cells coordinate the switch between Nbs1's effect on ATM activity and its engagement in downstream checkpoint signalling remains unclear. Better insight into this question may be provided by the emerging assays capable of dissecting the hierarchical and spatio-temporal organization of DNA damage response. For instance, it was shown that following its recruitment to the DSB-containing nuclear compartments, Nbs1 undergoes a dynamic exchange between the DSB sites and the neighbouring nucleoplasm (Lukas *et al*, 2003). A moderate (yet significant) increase in the affinity of Nbs1 for the damaged areas brings about the concentration of the 'activated' (ATM-phosphorylated) pool of Nbs1 in the vicinity of DNA lesions, thereby preventing its 'dilution' in undamaged parts of the nucleus. Thus, it appears that the dynamic accessibility of ATM-phosphorylated Nbs1 to DSB sites is essential for the biological roles of the MRN complex. However, the precise molecular determinants of the Nbs1's recruitment to, and the dynamic exchange at, the DSB sites remain unknown.

While ATM-mediated phosphorylation of histone H2AX (γ-H2AX) in chromatin regions surrounding a DSB does not constitute the initial DSB recognition signal for checkpoint

*Corresponding author. Danish Cancer Society, Institute of Cancer Biology, Strandboulevarden 49, 2100 Copenhagen, Denmark.
Tel.: +45 35 25 73 10; Fax: +45 35 25 77 21;
E-mail: lukas@biobase.dk
[4]Present address: Department of Genetics, The Institute of Life Sciences, The Hebrew University of Jerusalem, Jerusalem 91904, Israel

Received: 18 December 2003; accepted: 14 May 2004; published online: 17 June 2004

regulators (including Nbs1), it is required for their subsequent accumulation in the so-called IR-induced nuclear foci (IRIF) (Celeste *et al*, 2003). Furthermore, siRNA-based depletion of the 'checkpoint mediator' Mdc1/NFBD1 (Ozaki *et al*, 2000; Goldberg *et al*, 2003; Lou *et al*, 2003; Shang *et al*, 2003; Stewart *et al*, 2003; Xu and Stern, 2003a) prevented the accumulation of MRN components in IRIF (Goldberg *et al*, 2003; Stewart *et al*, 2003; Xu and Stern, 2003b). Although intriguing, these data did not elucidate the exact relationship between the γ-H2AX- and Mdc1-mediated controls over Nbs1 redistribution in response to DNA damage. Both Nbs1 and Mdc1 contain FHA and BRCT domains that interact with phospho-Ser or phospho-Thr residues such as those generated by ATM in the vicinity of DNA lesions (Ozaki *et al*, 2000; Desai-Mehta *et al*, 2001; Cerosaletti and Concannon, 2003; Goldberg *et al*, 2003; Lee *et al*, 2003; Shang *et al*, 2003; Stewart *et al*, 2003). Indeed, both proteins have been proposed to interact directly with γ-H2AX *in vitro* (Kobayashi *et al*, 2002; Stewart *et al*, 2003; Xu and Stern, 2003b). On the other hand, the bulk of Mdc1 could be immunodepleted from cell lysates with antibodies against the MRN core components, suggesting that Mdc1 might be a constitutive part of the MRN holocomplex (Goldberg *et al*, 2003). Thus, the key question is whether Mdc1, Nbs1, or both are required for the recognition of and productive interaction with γ-H2AX-modified chromatin. Furthermore, whether and how Mdc1 participates in the initial (γ-H2AX-independent) recruitment of Nbs1 to sites of DNA damage is unknown. Here, we address these issues by combining biochemical approaches with studies of DNA damage-induced redistribution of Mdc1 and Nbs1 in their physiological environment—the nucleus of a living cell.

Results

Recruitment kinetics of Nbs1 and Mdc1 to DSB-containing nuclear compartments

To circumvent technical limitations of the 'static' assessment of IRIF in fixed cells, we constructed an integrated imaging unit that combines microlaser-assisted generation of spatially defined DSB areas in mammalian cells with rapid, continuous and interactive image acquisition (Supplementary information 1). In addition, we generated a panel of cell lines derived from checkpoint-proficient human U-2-OS cells stably expressing Nbs1 or Mdc1 proteins tagged with green fluorescent protein (GFP) and/or its spectral variant, yellow fluorescent protein (YFP). The functionality and integration of these constructs into ATM- and/or MRN-controlled pathways have been characterized before (Lukas *et al*, 2003) and additional evidence is provided in this study. In brief, the chimeric proteins are expressed to near-physiological levels (Supplementary information 2), and retain their normal functions, including rapid recruitment to and a dynamic exchange at the sites of DSBs (Figures 1 and 2). Together with the ability of our system to assess simultaneously GFP- and YFP-tagged proteins in mixed cell populations, these tools enable an uninterrupted monitoring and direct comparison of intranuclear redistribution of Mdc1 and Nbs1 at a single-cell level, starting from a few seconds after DSB generation.

These real-time measurements revealed an extremely rapid accumulation of either protein around the laser-generated,

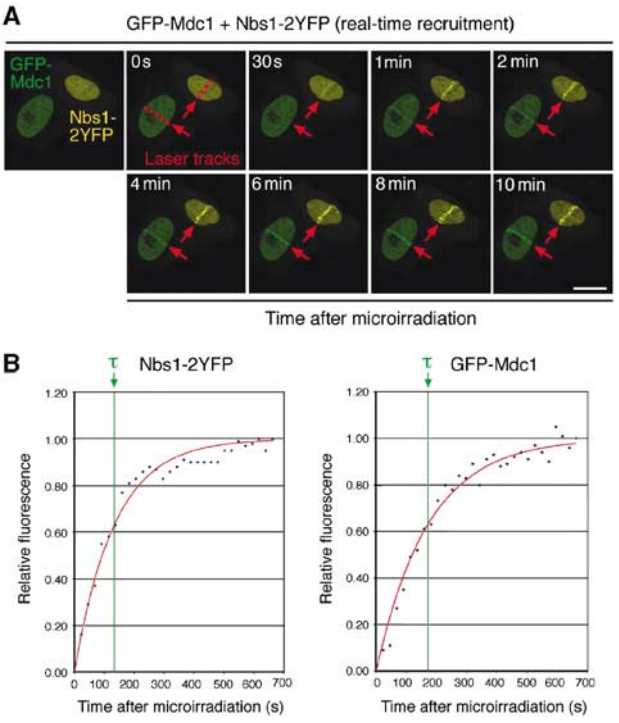

Figure 1 Real-time recruitment of Nbs1 and Mdc1 to the microlaser-generated sites of DNA damage. (**A**) U-2-OS cells expressing Nbs1-2YFP or GFP-Mdc1 were mixed (1:1) and co-cultivated for 24 h. The YFP and GFP signals were unmixed through the spectral analyser to discriminate the Nbs1- and Mdc1-expressing cells. The cells were microirradiated with a laser beam along 0.5–1-μm-wide tracks spanning the entire nuclear diameter, and the redistribution of the respective fluorophore-tagged proteins was recorded by a repeated scanning of the same field at 20 s intervals. Selected time points covering the earliest signs of Nbs1 and/or Mdc1 recruitment up to their stabilized interaction with DSB are shown. The arrows indicate the laser movement during microirradiation. Scale bars = 10 μm. (**B**) Kinetic curves of Nbs1 and Mdc1 recruitment to laser-generated, DSB-containing nuclear compartments. The data show examples of normalized data from one cell expressing Nbs1-2YFP and GFP-Mdc1, fitted to a model for the first-order response to a step change (step = DSB generation; Supplementary information 1). The value of the calculated recruitment time constant (τ) is indicated by a green line.

DSB-containing, subnuclear tracks (Figure 1A). The increase of Nbs1-2YFP- and GFP-Mdc1-associated fluorescence in the damaged nuclear regions became discernible already within 20–30 s (Figure 1A). Thereafter, both proteins underwent a rapid accumulation in the DSB regions, and reached a steady-state equilibrium by 8–10 min after laser exposure (Figure 1B). The recruitment of both proteins to DSBs exhibited the kinetics of a first-order response to a step change, implying that recruitment of Mdc1 and Nbs1 as a function of time-dependent DSB generation (step) is well described by a first-order linear differential equation (Figure 1B, and Supplementary information 1 for kinetics modelling). The kinetic parameter (τ) calculated after integrating measurements from multiple cells ($n = 18$) indicated that the kinetics of Mdc1 and Nbs1 recruitment to damaged chromosomal regions is very similar (Table I). Together, these measurements support the proposed functional link between Mdc1 and the MRN complex in DSB metabolism (see Introduction), and extend the previous biochemical and cytological studies by delineating the critical period from DSB generation to

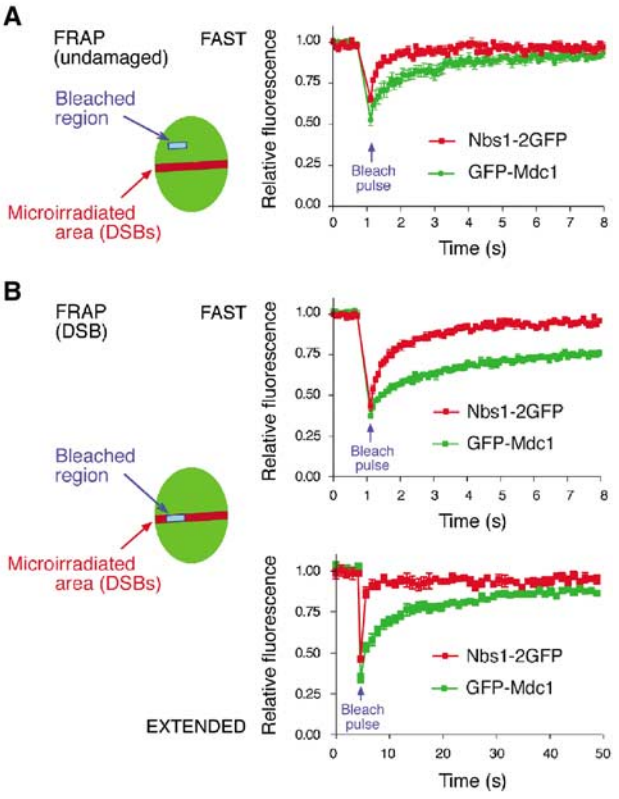

Figure 2 Distinct intranuclear movement of Nbs1 and Mdc1 before and after DNA damage. U-2-OS cells expressing Nbs1-2GFP or GFP-Mdc1 were microirradiated and 10 min later subjected to the FRAP analysis (Supplementary information 1). The positions of the microirradiated (red stripes) and the bleached regions (blue boxes) in undamaged nucleoplasm (**A**) and in the DSB-containing nuclear compartments (**B**) are schematically indicated. The total duration of image recording in the postbleached period is indicated by FAST (10 s) and EXTENDED (60 s). The latter protocol was used to achieve the maximum recovery of both Nbs1 and Mdc1 in the microirradiated nuclear compartments. The data integrate measurements form 10 independent cells for each nuclear location.

Table I Effective diffusion coefficient (D_{eff}), mean residence time (t_m), and recruitment time constant (τ) of Mdc1 and Nbs1

	Undamaged nucleoplasm	DSB	
	D_{eff} ($\mu m^2/s$)	t_m (s)	τ (s)
GFP-Mdc1	2.08 ± 0.29*	6.68[a]	195.23 ± 19.58**
Nbs1-2GFP	2.53 ± 0.30*	0.69[a]	177.42 ± 41.16[b],**

*$P = 0.0195$, **$P = 0.36$.
[a]See Supplementary information 1 for standard deviation of t_m and for mathematical processing of all measurements included in this table.
[b]Nbs1-2YFP.

stabilized equilibrium of the Nbs1 and Mdc1 interaction with the sites of DNA lesions. It seems plausible that this period spans most (if not all) critical events in terms of sensing and signalling the DNA damage.

Mdc1 undergoes partial immobilization in damaged nuclear compartments

We employed fluorescence recovery after photobleaching (FRAP), a method capable of resolving the dynamics of protein interactions with defined cellular structures on a subsecond scale (Supplementary information 1). To make the measurements of Nbs1 and Mdc1 mobility directly comparable, both proteins were tagged with GFP to avoid potential differences in photobleaching efficiency between GFP and YFP. Also, because of some cell-to-cell variability in the amount of the GFP-tagged proteins in our cell lines, only cells with GFP intensities comparable with approximately equimolar amounts of the GFP-tagged Mdc1 and/or Nbs1 and their endogenous counterparts (Supplementary information 2) were considered for FRAP analyses.

Surprisingly, despite the near-simultaneous recruitment of Nbs1 and Mdc1 observed in the real-time assays, the comparison of FRAP curves revealed notable distinctions. Most significantly, while the Nbs1-2GFP signal within the bleached regions placed in the undamaged nuclear compartments rapidly recovered to the prebleach values, the recovery of GFP-Mdc1 proceeded with a slower kinetics (Figure 2A) indicating several distinct populations moving at different rates. Indeed, calculation of the effective diffusion coefficients (D_{eff}; Essers *et al*, 2002; see Supplementary information 1) in undamaged nuclei revealed a slower diffusion rate of Mdc1 when compared to Nbs1 analysed under identical conditions (Table I). Together, these data indicate that without DNA damage the interaction between Nbs1 and Mdc1 is dynamic. The two proteins do not seem to migrate in preassembled holocomplexes, and Mdc1 (the slower-moving component) is likely involved also in interactions distinct from those with MRN.

Strikingly, after arrival at the DSB sites, the differences in mobility between Nbs1 and Mdc1 became even more pronounced. After the bleach pulse, the DSB-associated Nbs1-2GFP fluorescence rapidly recovered to the prebleach values, indicating that even after establishing contacts with the damaged sites the entire pool of the nuclear Nbs1-2GFP protein remained mobile (Figure 2B; also see Lukas *et al*, 2003). In contrast, a sizable fraction of GFP-Mdc1 became more durably associated with the microirradiated areas manifested by the lack of complete recovery of the GFP-Mdc1-associated fluorescence immediately after the bleach pulse (Figure 2B, top panel), and by a relatively slow kinetics in reaching the intensities close to the prebleach values (Figure 2B, bottom panel). Specifically, the mean residence time that Mdc1 spends bound to DSB was 6.68 s, a value nearly 10-fold higher compared to DSB-associated Nbs1 (Table I). Consistently, a parallel biochemical assay revealed that while the chromatin binding of Mdc1 substantially increased in the presence of DSBs, the ability of Nbs1 to interact with chromatin remained at the level observed in the nondamaged cells (compare the P2 fractions in Figure 5A). Hence, generation of DSBs has a differential impact on the dynamics of Mdc1 and Nbs1, causing a marked immobilization of the former while allowing rapid exchange of the latter.

Accumulation of Nbs1 in DSB-containing nuclear compartments requires Mdc1 including the earliest stages of the checkpoint response

To test whether Mdc1 modulates the dynamics of Nbs1 interaction with DSB sites, we applied the microirradiation/real-time imaging technique to cells in which endogenous Mdc1 had been depleted by RNA interference (RNAi). The efficiency of the Mdc1-targeting siRNA oligonucleotides was assessed by co-immunostaining of endogenous Mdc1 and

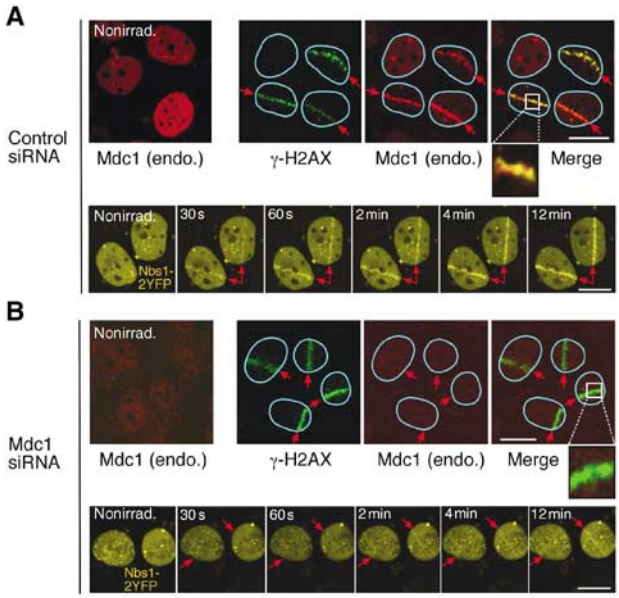

Figure 3 Decreased affinity of Nbs1 to the DSB-containing nuclear compartments in cells lacking Mdc1. U-2-OS cells were treated with control (**A**, top panel) and the Mdc1-targeting (**B**, top panel) siRNA oligonucleotides for 96 h. The nuclei were then subjected to local microirradiation, fixed 10 min later, and immunostained with antibodies to γ-H2AX (green) and total Mdc1 (red). The insets in (A, B) show a higher magnification of the respective microirradiated areas. In parallel, U-2-OS cells stably expressing Nbs1-2YFP were treated with control siRNA (A, bottom panel) or Mdc1-targeting siRNA (B, bottom panel) and analysed by the *in vivo* real-time recruitment assay as described in Figure 1. The arrows indicate the laser movement during microirradiation. Scale bars = 10 μm.

γ-H2AX, an established marker for DSBs in chromosomal DNA (Rogakou *et al*, 1999). In control siRNA-treated cells, Mdc1 underwent a quantitative relocalization from the diffuse pan-nuclear pattern to the laser-treated areas (Figure 3A, top) where it overlapped with γ-H2AX-decorated chromatin (Figure 3A, inset). This corresponded to a rapid and robust recruitment of Nbs1-2YFP to the DSB sites measured by the real-time recruitment assay (Figure 3A, bottom). In contrast, the Mdc1-specific siRNA depleted the protein to levels below immunochemical detection in both unstressed and microirradiated cells (Figure 3B, top). Under these conditions, the accumulation of Nbs1-2YFP in regions of DNA damage was grossly impaired, manifested by a barely discernible concentration of Nbs1-2YFP in the irradiated areas (Figure 3B, bottom, and Figure 7E for quantification). We conclude that Mdc1 is required for the normal accumulation of Nbs1 to regions of DNA damage, including the critical early stages of the DSB-evoked checkpoint response. Importantly, the lack of Nbs1 recruitment to DSBs in Mdc1-deficient cells occurred despite the productive phosphorylation of histone H2AX in the DSB-flanking chromosomal areas (Figure 3B).

Lack of Mdc1 causes dispersal of ATM-phosphorylated Nbs1 to undamaged nuclear compartments

The inability of Nbs1 to concentrate around freshly generated DSBs in Mdc1-deficient cells could be interpreted in two ways. Loss of Mdc1 might either totally uncouple Nbs1 from DSBs and/or DSB-generated structures, or it may allow initial DSB recognition but reduce the residence time of Nbs1 at such sites. To discriminate between these scenarios, we examined the distribution of ATM-phosphorylated Nbs1, a specific pool of the protein directly engaged in the DSB response. To this end, we employed phospho-specific antibodies to Ser-343 (S343), one of the prominent sites of Nbs1 phosphorylated by ATM (D'Amours and Jackson, 2002). In control cells, laser treatment triggered a marked accumulation of phospho-S343-associated fluorescence in the microirradiated areas and a moderate overall increase of the fluorescence signal throughout the nucleoplasm (Figure 4A). This is consistent with the dynamic exchange of Nbs1 at the damaged nuclear compartments (Figure 2B; Lukas *et al* 2003). Strikingly, while siRNA-mediated ablation of Mdc1 did not abolish cytologically detectable increase in Nbs1 phosphorylation, it prevented its accumulation in the microirradiated regions and allowed it to become dispersed throughout the nucleoplasm (Figure 4B). Similar results were obtained with other antibodies to phospho-S343 (unpublished results), and the normal kinetics of Nbs1 phosphorylation in Mdc1-depleted cells was validated by a time-course experiment in cells exposed to low-dose IR (Figure 4C).

The aberrant localization of Nbs1 in the Mdc1-depleted cells poses an important question of what are the spatial requirements for Nbs1 phosphorylation. Two scenarios could be envisaged. First, even in the absence of Mdc1, Nbs1 still requires a transient contact with DSBs for a productive enzyme–substrate interaction with ATM. Second, the lack of Mdc1 disrupts the physiological spatio-temporal requirements of ATM–Nbs1 interactions (restricted normally to DSBs) thereby allowing ectopic phosphorylation of the latter in undamaged nuclear compartments. To discriminate between these two possibilities, we employed a strategy similar to that used previously in studying Chk2 response to local DSBs (Lukas *et al*, 2003) and generated an immobile version of Nbs1-GFP by in-frame fusion with histone H2B, a constitutive component of mammalian chromatin (Supplementary information 3). Although present throughout the nucleus, the immobile Nbs1 was still phosphorylated only in the microirradiated areas even after quantitative downregulation of endogenous Mdc1 and detergent pre-extraction (the latter treatment was used to facilitate evaluation of the immobile Nbs1 without interference with the endogenous protein) (Figure 4D). These data suggest that the lack of Mdc1 does not impair the initial recognition of DSBs by Nbs1, and does not interfere with the productive enzyme–substrate interaction between Nbs1 and ATM at sites of DNA damage. Instead, the absence of Mdc1 precludes the ability of Nbs1 to gain physiological affinity for, and to concentrate within, the damaged nuclear compartments.

Depletion of Mdc1 or H2AX uncouples Nbs1 from sustained interaction with DSB-modified chromatin

To identify which structure(s) at or around DSBs serve as an 'anchor' for a sustained Nbs1 interaction, we took advantage of the fact that the engagement of Nbs1 with DSB compartments is accompanied by an increased resistance to extraction with mild detergent-containing buffers (Mirzoeva and Petrini, 2001; Lukas *et al*, 2003). We therefore reproduced the previous experiments after a short pre-extraction of the microirradiated cells before fixation and immunostaining. In control siRNA-treated cells, phosphorylated Nbs1 resisted extraction and the protein remained tightly associated with

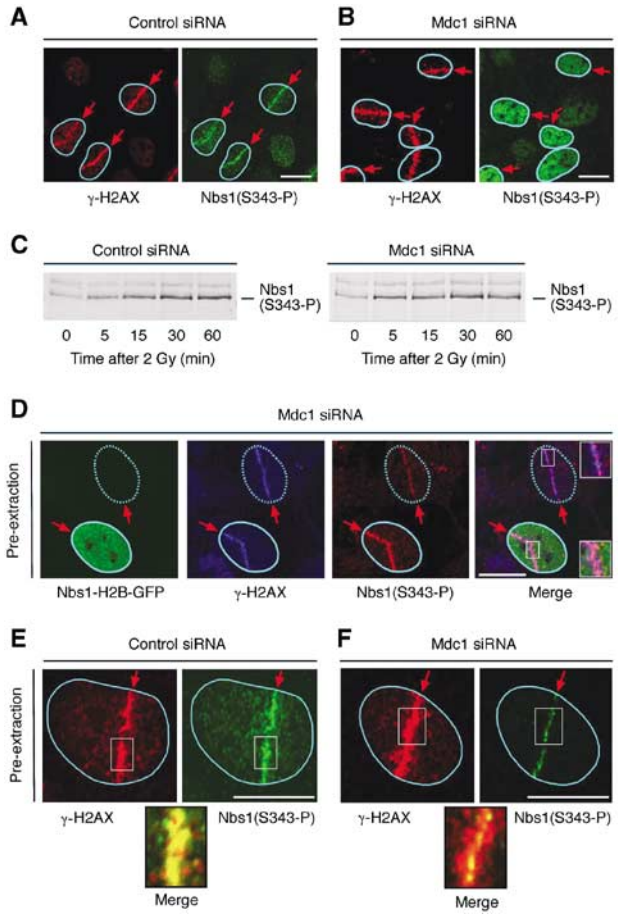

Figure 4 Impaired redistribution of ATM-phosphorylated Nbs1 in Mdc1-depleted cells. (**A, B**) U-2-OS cells were treated with control (A) and Mdc1-specific (B) siRNA oligonucleotides for 96 h, microirradiated, incubated for 10 min, fixed, and co-immunostained with phospho-specific antibodies to γ-H2AX and Nbs1(S343). (**C**) U-2-OS cells were transfected with control or Mdc1-specific siRNA duplexes for 96 h and exposed to IR (2 Gy). At the indicated time points, the cell lysates were analysed by immunoblotting with the phospho-specific antibody to Nbs1(S343). (**D**) U-2-OS cells were treated with Mdc1-specific siRNA oligonucleotides for 72 h, microinjected with the Nbs1-H2B-GFP expression plasmid (10 μg/ml), incubated for additional 36 h, pre-extracted to remove the bulk of endogenous Nbs1 (Materials and methods), fixed, and immunostained with the indicated antibodies. Note the stronger, DSB-restricted Nbs1-S343 phosphorylation in the cell nucleus expressing the immobile form of Nbs1 (marked by solid circle) compared to the neighbouring control nucleus (dashed circle). The insets show enlargements of the respective segments in the merged image. (**E, F**) U-2-OS cells were treated with control (E) or Mdc1-targeting (F) siRNA oligonucleotides, and microirradiated as in (A, B). After 10 min, the cells were pre-extracted for 5 min (Materials and methods), fixed, and co-immunostained with the indicated phospho-specific antibodies. The insets show magnified microirradiated fields. The arrows indicate the laser movement during microirradiation. Scale bars = 10 μm.

microirradiated, γ-H2AX-coated chromosomal areas (Figure 4E). In contrast, the bulk of the disseminated Nbs1 in Mdc1-depleted cells was quantitatively removed under these conditions (Figure 4F). Importantly, detergent extraction in Mdc1-deficient cells 'unmasked' a small fraction of phosphorylated Nbs1 in a form of microfoci randomly distributed along the centre of the microirradiated nuclear tracks (Figure 4F). Because no traces of endogenous Mdc1 were detected in the microirradiated regions (Figure 3B, inset), these structures likely reflect Mdc1-independent binding of Nbs1 to the physical sites of DSBs. Consistently, the previous real-time analyses of Nbs1 redistribution also revealed minute amounts of the total Nbs1-2GFP protein in the microirradiated areas even after Mdc1 depletion (Figure 3B, and Figure 7E for quantification). Most significantly, apart from these residual Nbs1 microfoci, the bulk of the γ-H2AX-decorated chromatin was largely free from phosphorylated Nbs1 (Figure 4F, inset). Thus, while ablation of Mdc1 does not seem to impair recognition of DNA breaks as such, it uncouples Nbs1 from the DSB-flanking chromatin and converts it into a more soluble protein despite prominent histone H2AX phosphorylation.

Two additional pieces of evidence support the above conclusions. First, downregulation of H2AX by siRNA prevented relocalization of endogenous Mdc1 to DSB sites (Figure 6A and B), triggered pan-nuclear dissemination of ATM-phosphorylated Nbs1 (Figure 6C and D), and impaired Nbs1 association with the DSB regions *in vivo*, as measured by the real-time recruitment assay (Figure 6E and F). Second, a complementary biochemical analysis of a HeLa cell line where the endogenous Mdc1 was stably knocked down by RNA interference (Materials and methods) revealed that the presence of Mdc1 is required to promote efficient binding of the MRN complex to phosphorylated peptides derived from the H2AX C-terminus (Figure 5B). Together, these data support and extend the notion that Mdc1 functions as a molecular linker between the ATM-generated phospho-epitopes on the DSB-modified chromatin and the sustained accumulation of the MRN complex within these regions.

Disruption of the Nbs1 FHA domain abrogates its interactions with DSB-flanking chromatin

To elucidate whether phosphorylation of Nbs1 by ATM and/or its ability to interact with other ATM-phosphorylated

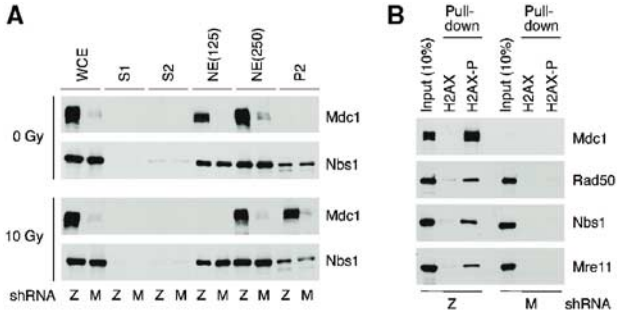

Figure 5 (**A**) Mdc1 but not Nbs1 chromatin binding increases upon induction of DSBs. HeLa cells stably expressing Mdc1-targeting (M) or a LacZ (Z) control shRNA were exposed to 10 Gy of IR. After 1 h, the cell lysates were fractionated (Materials and methods) to separate cytoplasmic (S1) and soluble nuclear (S2) proteins from chromatin. The chromatin pellet was subsequently washed with increasing salt concentrations (125 and 250 mM, respectively), and the remaining pellet (P2) was resuspended in SDS sample buffer and briefly sonicated to release the chromatin-bound proteins. All fractions were analysed by immunoblotting with antibodies to the indicated proteins. (**B**) Binding of MRN to γ-H2AX requires Mdc1. Nuclear extracts from HeLa cells stably expressing Mdc1-targeting (M) or a LacZ (Z) control shRNA were incubated with phosphorylated (H2AX-P) or nonphosphorylated (H2AX) peptides (Materials and methods). The bound proteins were analysed by immunoblotting with the indicated antibodies.

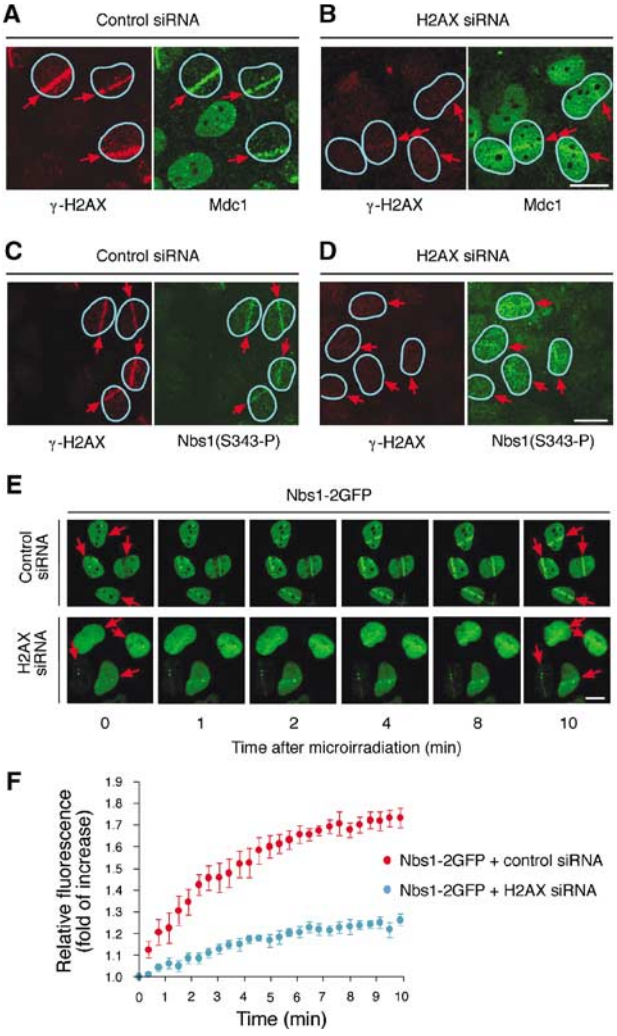

Figure 6 Transient ablation of H2AX impairs Mdc1 recruitment to DSBs and attenuates sustained interaction of Nbs1 with the damaged nuclear compartments. (**A, B**) U-2-OS cells were treated with control (A) and the H2AX-targeting (B) siRNA oligonucleotides for 96 h, microirradiated, and after additional 10 min fixed and co-immunostained with phospho-specific antibodies to γ-H2AX and total Mdc1. (**C, D**) U-2-OS cells were treated as in (A, B), and co-immunostained with phospho-specific antibodies to γ-H2AX and Nbs1(S343). (**E**) U-2-OS cells stably expressing Nbs1-2GFP were treated with control siRNA or H2AX-targeting siRNA as indicated and analysed by the *in vivo* real-time recruitment assay (Figure 1). The arrows indicate the laser movement during microirradiation. Scale bars = 10 μm. (**F**) Quantification of the real-time recruitment data obtained in (E). The graph integrates the data from 10 cells for each setting and shows the fold of increase of relative GFP-associated fluorescence in the microirradiated areas during the first 10 min after the laser treatment.

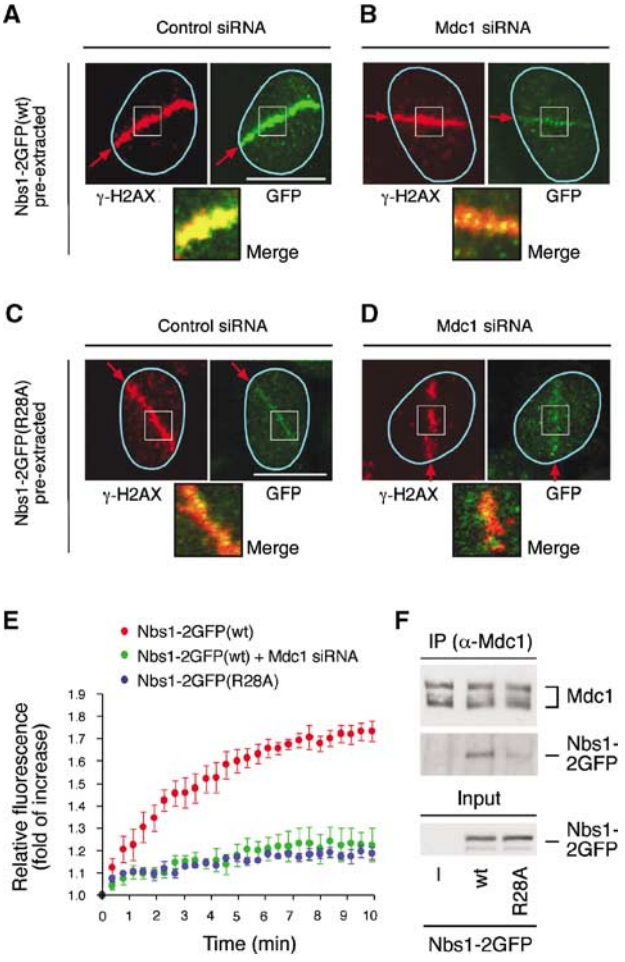

Figure 7 Disruption of the FHA domain uncouples Nbs1 from the γ-H2AX-modified chromatin regions. (**A, B**) U-2-OS cells stably expressing the wild-type (wt) form of Nbs1-2GFP were treated with control (A) or Mdc1-targeting (B) siRNA for 96 h, microirradiated, pre-extracted fixed after 10 min, and immunostained with phospho-specific antibodies to γ-H2AX. (**C, D**) U-2OS cells expressing the FHA-deficient (R28A) form of Nbs1-2GFP were treated with siRNA oligonucleotides as indicated and processed as in (A, B). (**E**) U-2-OS cells expressing the indicated forms of Nbs1-2GFP were microirradiated and subjected to the kinetic measurement of their DSB recruitment as described in Figure 1. Where indicated, endogenous Mdc1 was depleted by the siRNA oligonucleotides for 96 h before microirradiation. The graph integrates the data from 10 cells for each setting and shows the fold of increase of relative GFP-associated fluorescence in the microirradiated areas during the first 10 min after the laser treatment. (**F**) U-2-OS cells were transfected with expression plasmids coding for wild-type or R28A forms of Nbs1-2GFP. At 24 h after transfection, the cells were exposed to 2 Gy of ionizing radiation and cultured for additional 1 h. The cell lysates were immunoprecipitated with anti-Mdc1 antibody and immunoblotted with antibodies to Mdc1 or Nbs1 as indicated. The arrows indicate the laser movement during microirradiation. Scale bars = 10 μm.

proteins affects its DNA damage-induced redistribution, we generated U-2-OS cell lines stably expressing low levels of GFP-tagged Nbs1 mutants with the three ATM phosphorylation sites (S278, S343, S397) substituted by alanines (3 × A), and with a point mutation in the phosphate-binding FHA domain (R28A). These cells were microirradiated, pre-extracted before fixation, and analysed for their ability to bind DSBs and/or the neighbouring chromatin regions with or without concomitant downregulation of endogenous Mdc1.

Under these conditions, wild-type Nbs1-2GFP recapitulated the behaviour of the endogenous, ATM-phosphorylated Nbs1 (compare Figure 7A and B with Figure 4E and F). Thus, while in control cells the wild-type Nbs1-2GFP resisted detergent extraction throughout the microirradiated nuclear compartments (Figure 7A), Mdc1 depletion by siRNA prevented Nbs1-2GFP binding to the γ-H2AX-coated areas except for a small fraction of the protein scattered along the irradiated path (Figure 7B). The phosphorylation-deficient (3 × A) mutant behaved indistinguishably from the wild-

type protein (Supplementary information 4). In contrast, disruption of the FHA domain grossly impaired the ability of Nbs1 to accumulate within the γ-H2AX modified regions regardless of the presence of Mdc1 (Figure 7C and D). The recruitment of the R28A mutant (irrespective of the Mdc1 status) was reduced to a thin line of sub-micrometre foci along the laser path (Figure 7C and D). The size and intensity of these structures closely resembled the Nbs1-containing microfoci retrieved after detergent extraction of FHA-proficient forms of Nbs1 in Mdc1-depleted cells (Figure 4F; Supplementary information 4). Although the exact nature of these structures must await development of suitable cytological markers, we speculate that they represent the direct, chromatin-independent interaction of Nbs1 with DNA breaks. Consistent with the impaired affinity of the Nbs1(R28A) mutant to DNA damage-modified chromatin, the kinetics of its recruitment to the microirradiated areas was reduced to an extent that was very similar to the inefficient accumulation of wild-type Nbs1 in Mdc1-deficient cells (Figure 7E). Furthermore, the interaction of this FHA-deficient Nbs1 mutant with endogenous Mdc1 was markedly diminished compared to the wild-type Nbs1 (Figure 7F). Thus, the disruption of the Nbs1 FHA domain recapitulates the impact of Mdc1 deficiency on the ability of Nbs1 to undergo a sustained interaction with large chromosomal regions flanking the sites of DSBs.

Discussion

Several recent studies concluded that the MRN components do not form IRIF in the absence of Mdc1 (Goldberg *et al*, 2003; Stewart *et al*, 2003; Xu and Stern, 2003b). Our present work provides new insights into the Mdc1–MRN relationship by showing that only some—but not all—aspects of Nbs1's engagement with the DSB sites are regulated by Mdc1. First, through siRNA-mediated Mdc1 ablation and targeted immobilization of Nbs1 to chromatin, we provide evidence that Nbs1 phosphorylation does not occur stochastically in the undamaged nucleoplasm but requires interaction with ATM specifically at DSB sites. Together with our observation that in the absence of Mdc1 Nbs1 remains phosphorylated without being visibly tethered to the DSB regions, these data imply that both recognition of DSBs by Nbs1 and its productive interaction with ATM on these structures are rapid and transient events, and that neither of these processes require Mdc1 as a mediator. The modelling of kinetic properties of Mdc1 and Nbs1 derived from the FRAP measurements support this conclusion by showing that their interaction is dynamic and that Mdc1 is not a constitutive component of the MRN complex. Furthermore, our approaches identified a small fraction of Nbs1 within the damaged nuclear compartments that resisted detergent extraction. As no immunochemically detectable Mdc1 was found in these microfoci, these structures likely reflect Mdc1-independent interaction of Nbs1 directly with the DNA breaks. In a broader sense, elimination of Mdc1 'reduced' the complex spatio-temporal pattern of Nbs1 close to that described for the Chk2 kinase, another component of the ATM-controlled checkpoint program. We have previously shown that Chk2 (like Nbs1 in Mdc1-deficient cells) undergoes only a transient interaction with DSBs, from where—after phosphorylation by ATM—it rapidly spreads throughout the nucleus (Lukas *et al*, 2003). Hence, transient protein interactions (undetectable by cytologically discernible accumulation) appear to be sufficient for a direct interaction of checkpoint proteins with DNA breaks and for a productive communication between ATM and its substrates at DSB sites.

The second mode of Nbs1's interaction with damaged chromosomal regions strictly depends on Mdc1. Our data together with other evidence strongly suggest that Mdc1 represents a key molecular linker responsible for bridging Nbs1 with phospho-epitopes generated in DSB-flanking chromatin. Thus, Mdc1 localizes to the entire regions of the γ-H2AX-decorated chromatin *in situ* (Figure 3), it interacts with γ-H2AX *in vitro* (Stewart *et al*, 2003; Xu and Stern, 2003b) and, more specifically, Mdc1 directly binds H2AX peptides in a phosphorylation-dependent manner (Figure 5). Consistently, the recruitment of Mdc1 to IRIF requires the activity of the phosphatidylinositol-3-OH kinase-like family members (Goldberg *et al*, 2003; Stewart *et al*, 2003; Xu and Stern, 2003a). Furthermore, when physically uncoupled from Mdc1 (either through siRNA-mediated Mdc1 ablation or via mutation of its Mdc1-binding FHA domain), Nbs1 loses the ability to interact with DSB-surrounding chromosomal regions despite the fact that they contain γ-H2AX (Figures 3, 4 and 7). The latter *in vivo* observations were further supported by the *in vitro* binding assays revealing that MRN cannot bind phosphorylated H2AX peptides without a concomitant presence of Mdc1 (Figure 5). Collectively, these data are consistent with a model whereby Mdc1 functions as a molecular switch between the transient binding to DNA breaks by Nbs1 and its more durable accumulation within the flanking chromosomal regions delineated by the extent of ATM-mediated phosphorylation of H2AX. Only this latter mode manifests itself as a cytologically discernible protein accumulation (IRIF formation).

Consistent with this model, siRNA-mediated ablation of human H2AX recapitulated the impact of Mdc1 loss on Nbs1's ability to interact with the DSB-surrounding chromosomal areas (Figure 6). A recent study reported cytologically discernible accumulation of several DSB regulators around DSBs in mouse cells lacking H2AX in early stages after laser-generated DNA damage (Celeste *et al*, 2003). The differences in the extent of cytological manifestation of Nbs1's chromatin-independent interactions between our study and that of Celeste and co-workers likely reflect technical differences between the respective experimental systems. For instance, the density of DSBs in the microirradiated areas in sensitized mouse cells (Celeste *et al*, 2003) could be inherently higher than in human cells (this study), thereby making the former system more prone to see the transient interactions of proteins with a high number of closely neighbouring DNA breaks. Our system has been 'tuned down' to measure protein redistribution at the lowest possible laser energy that still elicits the DSB response (Supplementary information 1) thereby avoiding aggregation of excessive DNA damage in the microirradiated regions and allowing to discriminate between the low and high affinities of proteins to various DSB-associated structures. Regardless of these differences, our conclusions agree with the main findings of Celeste and co-workers in terms of a rapid recruitment of checkpoint proteins to DSBs independent of the H2AX phosphorylation. Our results extend these findings by showing that in human cells these chromatin-independent interactions are very

transient, do not cause readily detectable protein concentration, and are not restricted only to the earliest stages of the DSB response but rather coexist with the chromatin-mediated interactions until the efficient DSB repair.

The existence of two modes of Nbs1's interaction with damaged nuclear compartments (DSBs versus surrounding chromosomal areas) raises a question about their respective significance for the MRN functions. We show that while disruption of the FHA domain uncoupled Nbs1 from the γ-H2AX-modifed chromatin, it did not abolish interaction with structures resembling freshly generated and/or unrepaired DNA breaks (Figure 7). In this regard, it is important to note that a mutation in the FHA domain disrupted binding of Nbs1 to Mdc1 and, consistently, that the spatio-temporal defects of this mutant essentially recapitulated the aberrant behaviour of wild-type Nbs1 in Mdc1-deficient cells. Although the cellular phenotype caused by Mdc1 depletion is complex, one important aberration—an increased sensitivity to IR—is shared by cells with reduced Mdc1 and NBS cells reconstituted with the FHA-deficient forms of Nbs1 (Lee *et al*, 2003; Peng and chen, 2003; Stewart *et al*, 2003; Horejsi *et al*, 2004). Thus, it appears that the decreased survival of irradiated cells correlates with the inability of Nbs1 to undergo sustained, Mdc1-controlled engagement with the DSB surrounding chromosomal microenvironment.

It has been recently suggested that reduction of Mdc1 levels impairs activation of the ATM pathway (Mochan *et al*, 2003). In our hands, a detailed time-course approach revealed that quantitative depletion of Mdc1 by siRNA did not preclude efficient initiation of the ATM-controlled phosphorylation events (Supplementary information 5). Nevertheless, in some experiments, we did detect a moderate delay in the ATM auto-activation and in ATM-dependent Smc1 phosphorylation, indicating that while Mdc1 does not determine ATM activation *per se*, it can modulate the proper timing and velocity of the ATM-controlled checkpoint signalling (Supplementary information 5). The fact that the bulk of ATM activities remained preserved in Mdc1-deficient cells is consistent with our recent results showing that reconstitution of NBS cells with the FHA-deficient R28A mutant of Nbs1 (found here to mimic the lack of Mdc1 in terms of spatio-temporal aberrations) resulted in a near-complete restoration of ATM activation and phosphorylation of some of the tested ATM targets (Horejsi *et al*, 2004). Due to the relatively subtle impact of Mdc1 on the extent of ATM phosphorylations, we can envisage that the sustained (Mdc1-dependent) mode of Nbs1 interaction with the DSB-surrounding chromatin may not be restricted to the signalling and repair of the primary lesions. Even after the repair of the bulk of 'acute' DNA breaks is accomplished (which would lead to cancellation of the DSB-dependent recruitment of Nbs1), the continuous availability of the MRN complex might be necessary to secure restoration of the chromosomal architecture and other events ongoing in the vicinity of the original DNA lesions, such as recombination, replication, and chromatin remodelling. When combined, the timing, velocity, and efficiency of all these processes may, in a long run, increase the chance to restore the genome integrity in full thereby increasing the chances for survival after exposure to genotoxic stress.

Finally, our analyses revealed that despite their intimate link in DSB metabolism, the interaction between Nbs1 and Mdc1 is surprisingly flexible (Figure 2). The slower and more complex pattern of Mdc1's mobility in undamaged nucleoplasm indicates that it is likely engaged in interactions with proteins or nuclear structures that can compete with the MRN complex. The increased (and selective) immobilization of Mdc1 to chromatin after DSB generation (observed both by FRAP measurements and biochemical fractionation) raises the question of why the generation of DSBs increases the residence time of Mdc1 in the damaged nuclear regions while allowing Nbs1 to 'shuttle' rapidly between the DSB areas and the neighbouring nucleoplasm. The answer might be provided by several recent studies indicating that the 'mediator' role of Mdc1 is not restricted to the MRN complex. Mdc1 was reported to interact with other critical DSB-induced factors such as ATM, 53BP1, FANCD2, and Chk2 (Lou *et al*, 2003; Stewart *et al*, 2003; Xu and Stern, 2003b), and to colocalize in IRIF with others such as BRCA1 (Lou *et al*, 2003; Stewart *et al*, 2003). Thus, the more durable residence of Mdc1 in the damaged nuclear areas may generate the essential 'affinity platform' for a plethora of factors whose more dynamic exchange might be instrumental to adjust rapidly their respective concentrations at and around the DSBs according to the acute requirements of the ongoing repair processes.

Materials and methods

Plasmids

The Nbs1-2GFP expression plasmid has been described previously (Lukas *et al*, 2003). To generate Nbs1-2YFP, the tandem GFP cassette in the former plasmid was replaced by two in-frame linked units of YFP. The GFP/YFP-tagged phosphorylation-deficient (3 × A; Falck *et al*, 2002) and FHA-deficient (R28A; Horejsi *et al*, 2004) variants of Nbs1 were constructed as above. Chromatin-tethered Nbs1 was generated by in-frame insertion of the cDNA for histone H2B between the Nbs1 and the GFP moiety. The GFP-Mdc1 expression plasmids were gifts from Takashiro Nagase and Phang-Lang Chen (Ozaki *et al*, 2000; Shang *et al*, 2003).

Cell culture

Human U-2-OS osteosarcoma cells (ATTC) were transfected by Fugene 6 Reagent (Roche) with the expression plasmids containing the GFP/YFP-tagged Mdc1 and Nbs1 and the neomycin resistance gene. After selection with neomycin (G418, Invitrogen; 400 μg/ml), the resistant clones were tested for the expression and functionality of the GFP/YFP-tagged proteins. For live-cell experiments, the cells were plated on the Lab-Tek chambered coverglass (Nalge Nunc International). The culture medium was supplied with 10 μM 5′-bromo-2-deoxyuridine (BrdU; Sigma) for 24 h to presensitize the cells for the generation of DSBs after focal exposure to UVA light (Limoli and Ward, 1993; Supplementary information 1). This presensitization treatment by itself did not elicit any measurable DNA damage response (Supplementary information 6). Immediately before microirradiation, the cells were supplied with a phenol red-free, CO_2-independent medium (Invitrogen). Cells were placed into the XL 37°C-tempered incubator (Zeiss) mounted over the microscope stage. Nuclear microinjection of the expression plasmids was performed as described (Lukas *et al*, 2003).

RNA interference

The Mdc1-targeting siRNA duplexes were designed according to a previous report (Goldberg *et al*, 2003) and synthesized by Dharmacon Research. All experiments including Mdc1-directed RNAi were independently reproduced with the siRNA oligonucleotide described by Stewart *et al* (2003). The sequence for H2AX-targeting oligonucleotide was CAA CAA GAA GAC GCG AAU CdTdT. The control siRNA duplexes containing nonspecific sequences that do not have a match in human genome were provided by Dharmacon research (D-001205-01). Transfection of U-2-OS cells with the above siRNA oligonucleotides was performed with Oligofectamine (Invitrogen). Stable inhibition of the *Mdc1* gene was obtained in HeLa cells expressing in the retroviral vector

pSUPER-retro (Brummelkamp *et al*, 2002) a 19 nt sequence beginning at position 6142 of *Mdc1* mRNA (accession no. XM_376479). The sequence of the insert was 5′-gatccccgtctccca gaagacagtgattcaagagatcactgtcttctgggagacttttttggaaa-3′.

A control cell line was established by stable expression of siRNA corresponding to the gene encoding the LacZ protein in *Escherichia coli*. The insert in this construct was 5′-agcttttccaaaaagtctcccagaa gacagtgatctcttgaatcactgtcttctgggagacggg-3′.

Immunochemical techniques

The rabbit antibody to human Mdc1 has been described previously (Goldberg *et al*, 2003). Total Nbs1 was detected with a rabbit antibody (Ab398; Novus Biologicals). The phospho-Nbs1-Ser343 was detected by a rabbit antibody (3001; Cell Signalling Technology) and by a mouse monoclonal antibody (05-663; Upstate Biotechnology). Rabbit antibody (07-164) and mouse monoclonal antibody (05-636) to phospho-histone H2AX-Ser139 were from Upstate Biotechnology. Highly cross-absorbed secondary reagents for dual-colour detection (Alexa-488 and -568) were from Molecular Probes. Immunoblotting procedures (Falck *et al*, 2002) and isolation of chromatin-bound proteins (Mendez and Stillman, 2000) have been described previously. For peptide pull-down, biotinylated H2AX C-terminal peptides were synthesized at the Department of Biochemistry, University of Bristol, UK. The sequences were BIOTIN-SGSTVGPKAPSGGKKATQASQEY and BIOTIN-SGSTVGPKA PSGGKKATQAS(p)QEY, respectively. Peptides were coupled to streptavidin-coated Dynabeads M-280 (Dynal), incubated with the cell extracts in the presence of phosphatase inhibitors, washed with TBST, and resuspended in SDS sample buffer before loading on SDS–PAGE.

Microscopy

For immunofluorescence studies, cells grown on grid glass coverslips (Eppendorf) were fixed in 4% formaldehyde (15 min at room temperature), permeabilized in 0.2% Triton X-100 (5 min), and immunostained with the combination of antibodies specified in the figure legends. Where indicated, the cells were pre-extracted before fixation for 5 min at 4°C in the buffer containing 25 mM Hepes at pH 7.5, 50 mM NaCl, 1 mM EDTA, 3 mM $MgCl_2$, 300 mM sucrose, and 0.5% Triton X-100. Confocal fluorescence images were captured using a Zeiss LSM510 laser-scanning microscope. The construction of the integrated unit combining laser microirradiation with live-cell imaging together with description of real-time measurements of protein redistribution to local DSBs and the photobleaching analyses are described in detail in Supplementary information 1.

Supplementary data

Supplementary data are available at *The EMBO Journal* Online.

Acknowledgements

We thank Drs Phang-Lang Chen, Takashiro Nagase, and Yossi Shiloh for reagents, Claes Lindeneg, Per Geltzer, and Udo Buchwald for excellent technical assistance, and the Danish Cancer Society, Danish Cancer Research Foundation, European Commission, and John and Birthe Meyer Foundation for financial support.

References

Bakkenist CJ, Kastan MB (2003) DNA damage activates ATM through intermolecular autophosphorylation and dimer dissociation. *Nature* **421:** 499–506

Brummelkamp TR, Bernards R, Agami R (2002) A system for stable expression of short interfering RNAs in mammalian cells. *Science* **296:** 550–553

Carson CT, Schwartz RA, Stracker TH, Lilley CE, Lee DV, Weitzman MD (2003) The Mre11 complex is required for ATM activation and the G(2)/M checkpoint. *EMBO J* **22:** 6610–6620

Celeste A, Fernandez-Capetillo O, Kruhlak MJ, Pilch DR, Staudt DW, Lee A, Bonner RF, Bonner WM, Nussenzweig A (2003) Histone H2AX phosphorylation is dispensable for the initial recognition of DNA breaks. *Nat Cell Biol* **5:** 675–679

Cerosaletti KM, Concannon P (2003) Nibrin forkhead-associated domain and breast cancer C-terminal domain are both required for nuclear focus formation and phosphorylation. *J Biol Chem* **278:** 21944–21951

D'Amours D, Jackson SP (2002) The Mre11 complex: at the crossroads of DNA repair and checkpoint signalling. *Nat Rev Mol Cell Biol* **3:** 317–327

Desai-Mehta A, Cerosaletti KM, Concannon P (2001) Distinct functional domains of nibrin mediate Mre11 binding, focus formation, and nuclear localization. *Mol Cell Biol* **21:** 2184–2191

Dong Z, Zhong Q, Chen PL (1999) The Nijmegen breakage syndrome protein is essential for Mre11 phosphorylation upon DNA damage. *J Biol Chem* **274:** 19513–19516

Essers J, Houtsmuller AB, van Veelen L, Paulusma C, Nigg AL, Pastink A, Vermeulen W, Hoeijmakers JH, Kanaar R (2002) Nuclear dynamics of RAD52 group homologous recombination proteins in response to DNA damage. *EMBO J* **21:** 2030–2037

Falck J, Petrini JH, Williams BR, Lukas J, Bartek J (2002) The DNA damage-dependent intra-S phase checkpoint is regulated by parallel pathways. *Nat Genet* **30:** 290–294

Gatei M, Young D, Cerosaletti KM, Desai-Mehta A, Spring K, Kozlov S, Lavin MF, Gatti RA, Concannon P, Khanna K (2000) ATM-dependent phosphorylation of nibrin in response to radiation exposure. *Nat Genet* **25:** 115–119

Goldberg M, Stucki M, Falck J, D'Amours D, Rahman D, Pappin D, Bartek J, Jackson SP (2003) MDC1 is required for the intra-S-phase DNA damage checkpoint. *Nature* **421:** 952–956

Horejsi Z, Falck J, Bakkenist CJ, Kastan MB, Lukas J, Bartek J (2004) Distinct functional domains of Nbs1 modulate the timing and magnitude of ATM activation after low doses of ionizing radiation. *Oncogene* **23:** 3123–3128

Kim ST, Lim DS, Canman CE, Kastan MB (1999) Substrate specificities and identification of putative substrates of ATM kinase family members. *J Biol Chem* **274:** 37538–37543

Kobayashi J, Tauchi H, Sakamoto S, Nakamura A, Morishima K, Matsuura S, Kobayashi T, Tamai K, Tanimoto K, Komatsu K (2002) NBS1 localizes to gamma-H2AX foci through interaction with the FHA/BRCT domain. *Curr Biol* **12:** 1846–1851

Lee JH, Xu B, Lee CH, Ahn JY, Song MS, Lee H, Canman CE, Lee JS, Kastan MB, Lim DS (2003) Distinct functions of Nijmegen breakage syndrome in ataxia telangiectasia mutated-dependent responses to DNA damage. *Mol Cancer Res* **1:** 674–681

Lim DS, Kim ST, Xu B, Maser RS, Lin J, Petrini JH, Kastan MB (2000) ATM phosphorylates p95/nbs1 in an S-phase checkpoint pathway. *Nature* **404:** 613–617

Limoli CL, Ward JF (1993) A new method for introducing double-strand breaks into cellular DNA. *Radiat Res* **134:** 160–169

Lou Z, Chini CC, Minter-Dykhouse K, Chen J (2003) Mediator of DNA damage checkpoint protein 1 regulates BRCA1 localization and phosphorylation in DNA damage checkpoint control. *J Biol Chem* **278:** 13599–13602

Lukas C, Falck J, Bartkova J, Bartek J, Lukas J (2003) Distinct spatiotemporal dynamics of mammalian checkpoint regulators induced by DNA damage. *Nat Cell Biol* **5:** 255–260

Mendez J, Stillman B (2000) Chromatin association of human origin recognition complex, cdc6, and minichromosome maintenance proteins during the cell cycle: assembly of prereplication complexes in late mitosis. *Mol Cell Biol* **20:** 8602–8612

Mirzoeva OK, Petrini JHJ (2001) DNA damage-dependent nuclear dynamics of the Mre11 complex. *Mol Cell Biol* **21:** 281–288

Mochan TA, Venere M, DiTullio Jr RA, Halazonetis TD (2003) 53BP1 and NFBD1/MDC1-Nbs1 function in parallel interacting pathways activating ataxia-telangiectasia mutated (ATM) in response to DNA damage. *Cancer Res* **15:** 8586–8591

Ozaki T, Nagase T, Ichimiya S, Seki N, Ohiri M, Nomura N, Takada N, Sakiyama S, Weber BL, Nakagawara A (2000) NFBD1/KIAA0170 is a novel nuclear transcriptional transactivator with BRCT domain. *DNA Cell Biol* **19:** 475–485

Painter RB, Young BR (1980) Radiosensitivity in ataxia-telangiectasia: a new explanation. *Proc Natl Acad Sci USA* **77:** 7315–7317

Peng A, Chen PL (2003) NFBD1, like 53BP1, is an early and redundant transducer mediating Chk2 phosphorylation in response to DNA damage. *J Biol Chem* **278:** 8873–8876

Petrini JH, Stracker TH (2003) The cellular response to DNA double-strand breaks: defining the sensors and mediators. *Trends Cell Biol* **13:** 458–462

Rogakou EP, Boon C, Redon C, Bonner WM (1999) Megabase chromatin domains involved in DNA double-strand breaks *in vivo*. *J Cell Biol* **146:** 905–916

Shang YL, Bodero AJ, Chen PL (2003) NFBD1, a novel nuclear protein with signature motifs of FHA and BRCT, and an internal 41-amino acid repeat sequence, is an early participant in DNA damage response. *J Biol Chem* **278:** 6323–6329

Shiloh Y (2003) ATM and related protein kinases: safeguarding genome integrity. *Nat Rev Cancer* **3:** 155–168

Stewart GS, Wang B, Bignell CR, Taylor AM, Elledge SJ (2003) MDC1 is a mediator of the mammalian DNA damage checkpoint. *Nature* **421:** 961–966

Tauchi H, Matsuura S, Kobayashi J, Sakamoto S, Komatsu K (2002) Nijmegen breakage syndrome gene, NBS1, and molecular links to factors for genome stability. *Oncogene* **21:** 8967–8980

Uziel T, Lerenthal Y, Moyal L, Andegeko Y, Mittelman L, Shiloh Y (2003) Requirement of the MRN complex for ATM activation by DNA damage. *EMBO J* **22:** 5612–5621

van den Bosch M, Bree RT, Lowndes NF (2003) The MRN complex: coordinating and mediating the response to broken chromosomes. *EMBO Rep* **4:** 844–849

Xu X, Stern DF (2003a) NFBD1/KIAA0170 is a chromatin-associated protein involved in DNA damage signaling pathways. *J Biol Chem* **278:** 8795–8803

Xu X, Stern DF (2003b) NFBD1/MDC1 regulates ionizing radiation-induced focus formation by DNA checkpoint signaling and repair factors. *FASEB J* **17:** 1842–1848

Zhao S, Weng YC, Yuan SS, Lin YT, Hsu HC, Lin SC, Gerbino E, Song MH, Zdzienicka MZ, Gatti RA, Shay JW, Ziv Y, Shiloh Y, Lee EY (2000) Functional link between ataxia-telangiectasia and Nijmegen breakage syndrome gene products. *Nature* **405:** 473–477